CHEMISTRY OF MATERIALS

ARTICLE

pubs.acs.org/cm

A Molecular Precursor Approach to Tunable Porous Tin-Rich Indium Tin Oxide with Durable High Electrical Conductivity for Bioelectronic Devices

Yilmaz Aksu,[‡] Stefano Frasca,[§] Ulla Wollenberger,[§] Matthias Driess,*[,‡] and Arne Thomas*[,†]

[†]Institute of Chemistry: Functional Materials, Technische Universität Berlin, Englische Strasse 20, 10587 Berlin, Germany

[‡]Institute of Chemistry: Metalorganics and Inorganic Materials, Technische Universität Berlin, Strasse des 17, Juni 135, 10623 Berlin, Germany

[§]Institute of Biochemistry and Biology: Molecular Enzymology, University Potsdam, Liebknechtstrasse 24-25, 14476 Golm, Germany

Supporting Information

ABSTRACT: The preparation of porous, i.e., high surface area electrodes from transparent conducting oxides, is a valuable goal in materials chemistry as such electrodes can enable further development of optoelectronic, electrocatalytic, or bioelectronic devices. In this work the first *tin-rich mesoporous* indium tin oxide is prepared using the molecular heterobimetallic single-source precursor, indium tin tris-*tert*-butoxide, together with an appropriate structure-directing template, yielding materials with high surface areas and tailorable pore size. The resulting mesoporous tin-rich ITO films show a high and durable electrical conductivity and transparency, making them interesting materials for hosting electroactive biomolecules such as proteins. In fact, its unique performance in bioelectronic applications has been demonstrated by immobilization of high amounts of cytochrome c into the mesoporous film which undergo redox processes directly with the conductive electrode material.

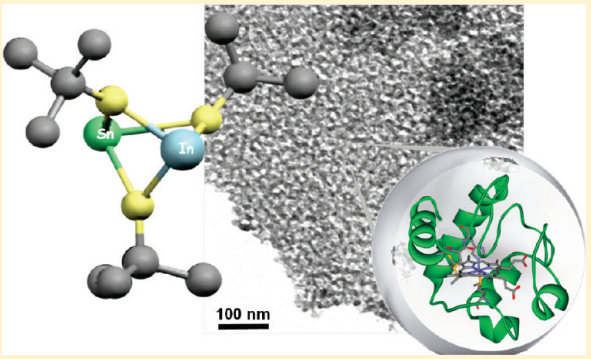

KEYWORDS: indium tin oxide ITO, electrode, bioelectrochemistry, device, cytochrome c

INTRODUCTION

Mesoporous metal oxides combine the unique features of mesoporosity, namely, small pores and high surface areas, with the versatile functions of metal oxides, for example, (semi)-conductivity, magnetism, photoluminescence, or catalytic activity.[1,2] They are commonly prepared by sol−gel routes using suitable templates as porogens,[3,4] yielding however amorphous pore walls in the first step, which restricts the range of application for most metal oxides.[5] Crystallization of the pore walls at higher temperatures, however, frequently results in structural collapse and consequently a substantial loss in porosity. In the case of ternary metal oxides, crystallization can even yield phase separation of the two binary metal oxides. For indium tin oxide (ITO), the most widely used transparent conducting oxide (TCO),[6,7] unfortunately all these obstacles apply and therefore the introduction of well-defined mesoporosity under retention of high conductivity is rather difficult. However, to prepare a mesoporous ITO would have certain advantages: First, the surface area would be reasonably increased, allowing the immobilization of higher amounts of electroactive species per electrode area. Furthermore, an organized mesostructure might facilitate electron transport toward electroactive centers. These features may enable further development of optoelectronic devices from dye-sensitized solar cells to electrochromic windows and could also be useful in electrocatalytic or bioelectronic devices including biosensors and biofuel cells.

One approach to increase the surface area of an ITO electrode is the deposition of ITO on porous glass substrates[8,9] or carbon nanotubes.[10] Only a few template-assisted preparations of porous ITOs have been reported, yielding powders with low conductivity[11] and/or with irregular porosity resulting from the loose packing of crystallites.[12,13] Smarsly and co-workers have synthesized ITO and other TCO films with 3D mesoporous architecture and appreciable conductivity using an improved structure-directing polymer template and a controlled tempering protocol.[14,15] This mesoporous ITO showed to be a suitable electrode for incorporation of a high amount of electroactive biomolecules.[16] Also, preformed TCO nanocrystals have been used to prepare mesoporous TCO films.[17]

A conceptual problem of all these approaches is further the limited amount of tin, which, although the cheaper component, is only slightly soluble in the In_2O_3 phase, typically around 1−10 wt %. Indeed, the solubility limit of Sn in In_2O_3 strongly depends on the particle size and temperature.[18] To avoid phase

Received: October 27, 2010
Revised: January 27, 2011
Published: March 04, 2011

Scheme 1. Structure of $In(O^tBu)_3Sn$ (ITBO)

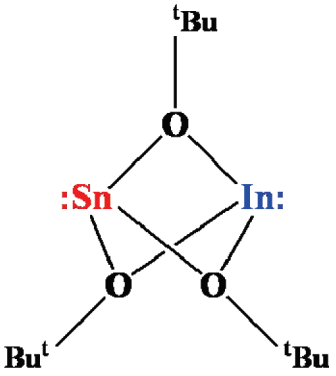

segregation of *tin-rich* ITO, a low-temperature approach with high control over the In/Sn molar ratio is required.

Recently, some of us reported on the molecular single-source precursor (SSP) indium tin tris-*tert*-butoxide (ITBO; Scheme 1) containing indium and tin in the molar ratio of 1:1, which facilitates the formation of tin-rich ITO with an identical stoichiometry in the final product.[19] Most importantly, the resulting tin-rich ITO shows high conductivity and transparency even in an amorphous state. Using such a SSP[20−25] thus could be a key to overcome all of the aforementioned problems regarding the template-assisted approach toward mesoporous ITO. As the ITBO precursor enables the formation of transparent conducting films without any crystallization step, the main cause of pore collapse of mesoporous metal oxides is excluded in these materials. Thus, ITBO appeared as highly suitable for the preparation of mesoporous, tin-rich ITO films with reliable high electrical conductivity and transparency using different templates.

EXPERIMENTAL SECTION

Preparation of Mesoporous, Tin-Rich ITO Films. ITBO was prepared and characterized according to published procedures.[19,26] Blends of KLE, F127, and Brij700 with ITBO were prepared by dissolving them in dry tetrahydrofurane (KLE) or dry toluene (F127 and Brij700) at ambient temperature and under nitrogen atmosphere. In a typical procedure, a KLE−ITBO solution was prepared by mixing a KLE (155 mg) solution in tetrahydrofurane (1 mL) with the appropriate amount of ITBO (620 mg) in tetrahydrofurane (1 mL) and stirred for 1 h at room temperature.

The glass substrates were cleaned in an ultrasonic cleaner for 10 min with acetone and isopropanol, respectively. The substrates were dried in a high-purity nitrogen gas stream just before use. To increase the compatibility of the substrate with the ITBO−polymer mixture and ameliorate the final film quality, the glass substrates were first coated with a solution of pure ITBO in toluene. Tin-rich ITO−polymer films were fabricated by spin coating the solutions of the corresponding ITBO−polymer mixtures under nitrogen atmosphere in a glovebox (<1 ppm H_2O and <1 ppm O_2). The coatings were aged for 30 min in nitrogen and then annealed for 2 h in air at different temperatures between 300 and 600 °C (ramp 5 °C min^{-1}). After heat treatment all samples were subsequently annealed at 300 °C in a reductive gas mixture (H_2/N_2:10%/90%, ramp 5 °C min^{-1}) for 90 min.

Four-Point Probe Measurements. The electrical resistivity was measured using the four-point probe method at room temperature, for which the instrument was assembled using a Keithley nanovoltmeter and a Keithley 2400 constant current source. UV/vis spectra were recorded using a Perkin-Elmer Lambda 20 spectrometer equipped with a reflecting sphere, Labsphere RSA-PE-20. Scanning electron microscopy (SEM) images were acquired using an Hitachi S-4000 microscope equipped with an SAMX EDX detector. Energy-dispersive X-ray spectroscopy using a CAMECA Camebax microbeam electron microprobe was employed to determine the quantitative chemical composition of the particles with a sample current of 18 nA at 15 kV. Transmission electron microscopy (TEM) images were taken with a Zeiss EM 912 Ω at an acceleration voltage of 120 kV. For the TEM measurements the films were scratched off from the substrate and transferred to a carbon-coated copper grid. Nitrogen sorption experiments were conducted at 77 K using an Autosorb-1 from Quantachrome Instruments. Before sorption measurements, the samples were degassed in vacuum overnight at 80 °C. The surface area was calculated from multipoint BET plot, and the pore volume was determined by the BJH method.

Electrochemistry. The electrochemical measurements were carried out with a Gamry Reference 600TM potentiostat (Gamry, USA) and performed in a homemade three-electrode cell with a total volume of 1 mL employing a platinum wire as the counter electrode, and an Ag/AgCl (1 M KCl) reference electrode, against which all potentials are reported, and the mesoporous ITBO-coated glass slide as working electrode with a circular surface of 5.5 mm in diameter. The mesoporous tin-rich ITO was employed as received without any further pretreatments. The system was equilibrated 1 h with the corresponding buffer solution before the measurement. The heterogeneorous electron transfer rate constants (k^0) were determined from cyclic voltammetric (CV) peak separation (ΔE_p) for scan rates ranging from 0.01 to 0.1 V s^{-1} using the method of Nicholson.[27]

For spectroelectrochemical experiments a homemade electrochemical cell equipped with a quartz window was incorporated into the sample compartment of a Beckman DU 640 spectrophotometer whereas the applied potential was controlled by a Gamry Reference 600TM potentiostat. The transmission spectra were recorded through one ITO-coated glass and the quartz glass. The amount of cytochrome c accommodated in the ITO was determined spectroscopically based on the extinction coefficients (ε) of 106100 M^{-1} cm^{-1} (410 nm) and 129100 M^{-1} cm^{-1} (416 nm) of ferric and ferrous cytochrome c, respectively.[28,29]

Immobilization of cytochrome c (horse heart, Sigma, Germany) was achieved by dipping ITO slide into a protein solution (15 μM in 5 mM potassium phosphate buffer solution, pH 7.0) at 4 °C. Prior to all the experiments, the supernatant cytochrome c containing solution was removed and the cell was rinsed and stirred for 1 min in a fresh buffer solution. The modified electrode was stored in buffer solution at 4 °C in a refrigerator until use.

RESULTS AND DISCUSSION

The ITBO precursor[26] (Scheme 1) can be prepared as a pale yellow crystalline solid in multigram scale through an improved literature procedure.[19] ITBO can be dissolved in a variety of solvents and plane ITO films can be produced from these solutions by spin- or dip-coating techniques. The mesoporous ITO films were produced from the ITBO precursor dissolved either in tetrahydrofurane or toluene and block-co-polymers as structure-directing templates, namely, poly(ethylene-*co*-butylene)-*b*-poly(ethylene oxides) (KLE),[30] Pluronic F127, and Brij 700. The precursor and the template were mixed together in the respective solvents and these solutions were spin-coated on glass substrates.

For nitrogen sorption experiments higher amounts of the materials were prepared by pouring the solutions into Petri dishes to produce larger and thicker films. Indeed, the amorphous nature of the resulting materials should in principle allow even

dx.doi.org/10.1021/cm103087p |*Chem. Mater.* 2011, 23, 1798–1804

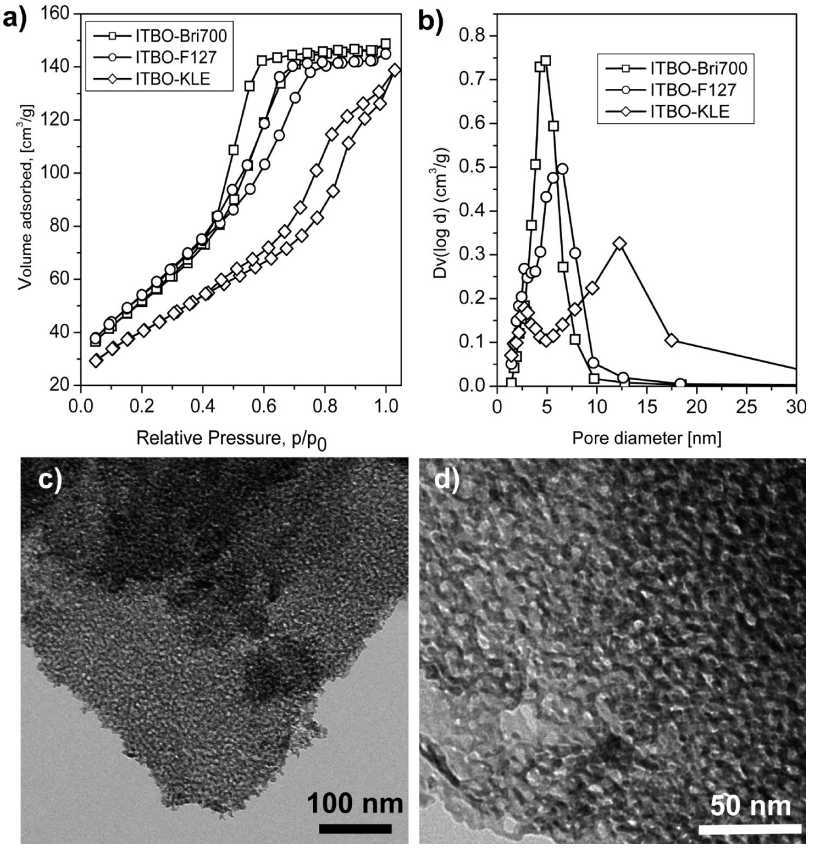

Figure 1. (a) Nitrogen sorption isotherms and (b) BJH pore size distribution of mesoporous ITOs prepared from the molecular precursor ITBO and KLE, F127, and Brij700 as templates, respectively. (c,d) TEM pictures of mesoporous tin-rich ITO templated with block-co-polymer KLE, at lower and higher magnification, respectively. Samples were calcined at 500 °C.

the preparation of monoliths. All these procedures were carried out under a controlled inert atmosphere in a glovebox.

ITBO is air-sensitive and readily polymerizes to give amorphous ITBO−polymers at ambient temperature when exposed to oxygen and humidity. Thus, no acid, base, or other additive had to be present in ITBO solutions to produce amorphous tin-rich ITO. The condensation process is thus quite different from the usually used sol−gel-approach, where adjustment of pH and water content is often crucial for the progress of the condensation of the metal−organic precursors. The resulting ITBO−polymer composite films in the presence of templates remain transparent (Figure S1 and Figure S2 in the Supporting Information) after exposure to air atmosphere, showing that no macrophase separation of the block-co-polymers from the ITBO phase occur during the condensation process. Removal of the templates was achieved by calcination at different temperatures. All films showed a homogeneous distribution of indium, tin and oxygen as determined by SEM-EDS elemental mapping. (Figures S3−S6 in the Supporting Information).

At first, a KLE block-co-polymer was used to probe whether mesoporous structures can be prepared using the ITBO precursor for tin-rich ITO. KLE block-co-polymers have shown to be useful templates for the generation of mesoporous silica and a variety of metal oxides[30−34] and also for the preparation of mesoporous ITO from conventional precursors.[14] Thus, KLE template and ITBO precursor were mixed in tetrahydrofurane in a 1:5 weight ratio (denoted ITBO_KLE). After film formation, removal of the template by calcination was carried out at different temperatures, namely, 400, 500, and 600 °C, to investigate the thermal stability of the resulting mesostructure.

Table 1. Porous Characteristics of Mesoporous Tin-Rich ITOs

sample	calcination temperature	surface area (m^2/g)	pore diameter (nm)	pore volume (cm^3/g)
ITBO_KLE	400 °C	149	12.3	0.21
ITBO_KLE	500 °C	126	12.5	0.20
ITBO_KLE	600 °C	44	12.6	0.11
ITBO_F127	400 °C	200	6.5	0.22
ITBO_Brij700	400 °C	190	4.8	0.23

The BET isotherms of the sample ITBO_KLE calcined at different temperatures show a type IV nitrogen sorption isotherm indicative of mesoporous materials (Figure 1 and Figure S7). Surface areas of 149, 124, and 44 m^2/g, were found for samples calcined at 400, 500, and 600 °C, respectively (Table 1). The decrease in the surface area shows that collapse of the mesostructure also occur to some extent for the here described materials, however, mainly at temperatures around 600 °C. For all samples pore diameter of ∼12 nm were calculated using the BJH method on the adsorption branch. The pore size is comparable to those of mesoporous silica and metal oxides prepared with the KLE template.[30]

Further insight into the pore structure was gained by TEM measurements (Figure 1c,d and Figure S8). A well-defined,

dx.doi.org/10.1021/cm103087p |*Chem. Mater.* 2011, 23, 1798–1804

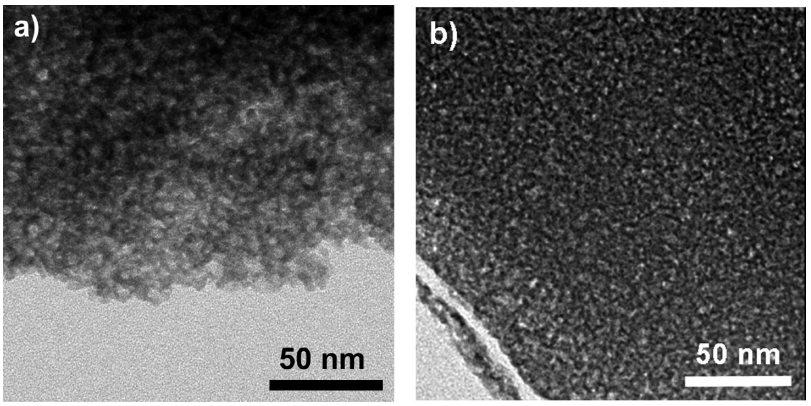

Figure 2. TEM images of mesoporous tin-rich ITOs templated with (a) Brij700 and (b) F127, respectively. Samples were calcined at 500 °C.

although disordered, porosity homogeneously distributed over the entire film can be observed at lower magnifications. At higher magnifications spherical mesopores with narrow pore size distribution are visible.

From the observed mesostructure some assumptions on the structural evolution of the organic−inorganic composites during preparation can be drawn. At first, it should be mentioned again that in the here described system no water is added during synthesis, which would allow the formation of micelles and subsequently lyotropic phases from the block-co-polymer. In contrast, in the preceding mixture the rather hydrophobic ITBO precursor and the organic solvent should rather impede the formation of supramolecular structures from the block-co-polymer. Pore size and pore structure of the resulting tin-rich ITOs are, besides the missing long-range order of the pores, nevertheless quite comparable to those found for mesoporous silicas templated with the same block-co-polymer.[30] Therefore, it can be ascertained that, also in the present system, micelles of the block-co-polymer have been replicated into the material. However, micelle formation probably just occurs at the last stage of formation of the material, that is, when the films are exposed to the atmosphere and humidity and the ITBO precursor starts to transform into tin-rich ITO. Thus, the irregular pore structure might show a kinetically trapped, that is, metastable, phase of the micellar superstructure.

The versatility of the here shown approach was tested by using two more, this time commercially available, surfactants (Brij700) and block-co-polymers (Pluronic F127), respectively. Because it was observed that better films of ITO can be produced when casted from toluene, the solvent was changed from tetrahydrofurane to toluene accordingly, although the aforementioned obstacles for the formation of lyotropic phases count even more in these systems. Remarkably, still mesoporous tin-rich ITOs with well-defined porous structures can be produced with both the templates (Figure 2, Table 1).

In a comparison of the BET isotherms and BJH pore size distributions for the ITO materials prepared from the templates Brij700, F127, and KLE, an increase in the pore size can be observed, from Brij700 with an average pore diameter of 4.8 nm to F127 with 6.5 nm to KLE with 12.3 nm. Thus, control and tailoring of pore size and structure of a mesoporous tin-rich ITO can be achieved. The TEM pictures of the mesoporous tin-rich ITOs prepared with Brij700 and F127 as template again show homogeneous yet disordered pore systems (Figure 2).

However, besides the control of the mesostructure, for the formation of TCOs obviously the conductivity is of main importance. The high solubility of the ITBO precursor in common aprotic organic solvents gives the unique opportunity to directly process from the precursor in solution without any additive or stabilizer. This approach leads to highly conductive, homogeneous, and compact thin films, superior to other applied methods.

Table 2. Sheet Resistance of the Best Mesoporous Films ITO−KLE and ITBO−F127 Samples and the Nonporous Film Prepared from Pure ITBO[a]

sample	film thickness (μm)	four-point resistivity (Ω/square)	sheet resistivity (Ω-cm)
ITBO_KLE	0.7	91.32	0.639×10^{-2}
ITBO_F127	1.5	115.02	1.725×10^{-2}
ITBO	2.0	20.49	0.410×10^{-2}

[a] All films were tempered at 400 °C in air and further annealed at 300 °C in a reductive gas mixture (H_2/N_2:10%/90%).

The mesoporous films were prepared by spin coating toluene solutions of ITBO−polymer mixtures on glass substrates under controlled conditions, for example, in nitrogen atmosphere (O_2 < 1 ppm, H_2O < 6 ppm) followed by thermal treatment in air at 400 °C and subsequently annealing at 300 °C in a reductive gas mixture (H_2/N_2:10%/90%) for 90 min. The morphology and electrical properties of the as-deposited films were very similar for each series (ITBO−KLE and ITBO−F127 system), confirming the high reproducibility of the technique employed. All the films prepared were transparent and showed very smooth morphologies. However, partially cracked films were observed for a few layers with increased film thickness during annealing. The transmission characteristics of the porous tin-rich ITO films were studied by UV−visible spectrometry (see Figure S1 and Figure S2 in the Supporting Information). The films show 70−75% optical transmission in the visible range, which even enables applications in printable electronics.

Electrical characterization of the as-prepared mesoporous, tin-rich ITO films by four-point probe measurements revealed remarkably low sheet resistivity of 91.32 Ω/square for the ITBO−KLE and 115.02 Ω/square for the ITBO−F127 system (see Table 2).

The approximate thickness of the as-deposited tin-rich ITO films was estimated by SEM studies to determine the electrical conductivity of the mesoporous coatings. The estimated width of the layer is about 750 nm for the ITBO−KLE and 1.5 μm for ITBO−F127 system on average (Figure 3). Assuming that the

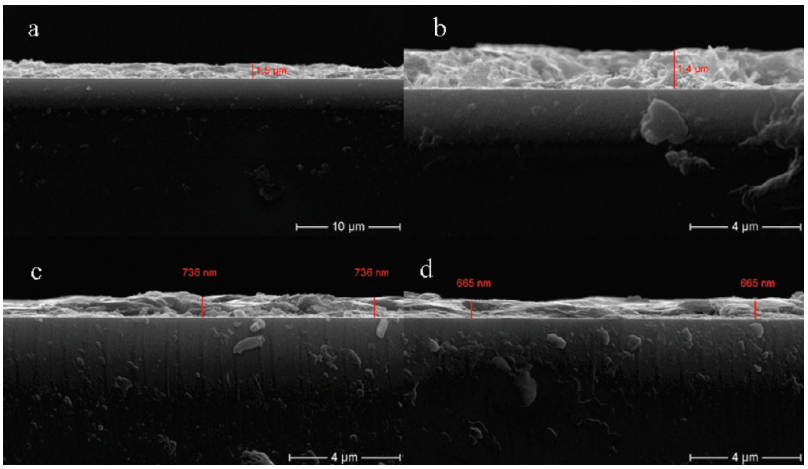

Figure 3. Cross-sectional SEM images of mesoporous, tin-rich ITO prepared with the molecular single-source precursor ITBO, using 20 wt % (a, b) F127 and (c, d) KLE as templates, respectively.

thickness of the films is uniform, the specific resistivity of the films was calculated by multiplying the sheet resistance determined by four-point probe measurements on the film thickness (see Table 2). With these values taken into account, the resistivity is on the order of 6.390×10^{-3} Ω-cm (ITBO−KLE) and 1.725×10^{-2} Ω-cm (ITBO−F127), respectively. In contrast, the resistivity of the porous film deposited with Brij700 is much higher, which can be attributed to the poor film quality and high roughness, apparently owing to the low adhesion of the ITBO−Brij700 mixture to the glass substrates.

Despite their high porosities, the ITBO/KLE and ITBO/F127 system lead to layers with high electrical conductivity, confirming the positive contribution of their nanostructures to their electrical properties.[35a] The morphology and nanostructure of the film possess great influence over the electrical conductivity of the coatings while they can affect the density and mobility of the carriers present in the layer material.[35−37] The modification of the dense tin-rich ITO films to layers with high porosity results in an increase of the oxygen vacancy (donor centers) density, which is partially reduced through the oxidation process in air and can thereby compensate the loss in conductivity during the heat treatment under oxidative conditions.

The best films were obtained at 400 °C, which is lower than the temperature used for thin film fabrications with commercially available ITO, which is generally synthesized at higher temperatures ($T > 550$ °C). This is the minimum temperature which is necessary for the complete degradation of the polymer additives to obtain coatings without carbon impurities. However, the resistivity of the mesoporous tin-rich ITO layers drastically decreases with increasing the annealing temperature ($T > 400$ °C). This can be related to improvements in the crystalline character of the coatings, leading to a decrease of donor sites trapped at the grain boundaries, and also to the out-diffusion of oxygen atoms from interstitial positions.[35−37] The durability of the electronic properties of the mesoporous tin-rich ITO films is considerably higher in comparison to those prepared from commercially available ITO. After the films ages in air for 3 months at room temperature, no significant change was observed in the conductivity.

The possibility to control and tailor the accessible mesoporosity, combined with the good electrical conductivity over a broad potential window and optical transparency, makes the mesoporous tin-rich ITO films an ideal material for hosting electroactive biomolecules such as proteins and thus an attractive alternative to other mesostructured TCOs.[16,28,38−43] This is of particular importance for the understanding of underlying redox processes in biomolecules and further for the development of bioelectronic devices including biosensors and biofuel cells. The major challenges for a successful application of redox proteins in bioelectronic devices is lifetime and effective interfacial electrochemical reactions of a sufficiently high amount of responsible biomolecules. Fast direct heterogeneous electron transfer between redox proteins and electrodes is often achieved after oriented assembly at appropriately modified surfaces using self-assembled monolayers or polyelectrolytes. The amount of immobilized protein is however limited to monolayer coverage.[44,45] This restriction has been circumvented by introduction of multilayer assemblies[46] and three-dimensional conductive matrixes.[47] ITO has a favorable negative excess surface charge,[48] which enables the electrostatic attraction of cationic proteins such as cytochrome c. The large surface area of the porous material allows the incorporation of high amounts of proteins. Voltammetry with optical spectroscopy can then be applied to study the effect of distinct potential trigger within a single sample to gain information about underlying redox processes.

Initial electrochemical experiments show a fast reduction and oxidation of the small mobile redox mediator $Ru(NH_3)_6^{2+/3+}$ with standard rate constants ($4 \pm 1 \times 10^{-3}$ cm s^{-1}) much higher than those for a crystalline mesoporous ITO, produced from conventional tin and indium precursors ($5 \pm 1 \times 10^{-4}$ cm s^{-1}).[14,16]

Equilibration of a mesoporous tin-rich ITO electrode in an aqueous solution of cytochrome c solution results in an efficient surface interaction of the protein, as revealed by the CVs that displayed a reversible response at low scan rate, with a formal potential of -6 ± 5 mV (vs Ag/AgCl/1 M KCl). A 15 μM cytochrome c concentration in the initial solution was selected as the optimum value to use for incubation. Assuming a spherical shape for cytochrome c with a surface area of ca. 7 nm^2,[28] the spectroscopic characterization of the immobilized protein reveals a higher protein loading of the ITBO_KLE ($\Gamma_{Cyt\_c} \sim$ 1900 pmol cm^{-2}, ~ 0.7 nm film thickness) than the ITBO_F127 ($\Gamma_{Cyt\_c} \sim$ 2400 pmol cm^{-2}, ~ 1.5 nm film thickness)), taking into account the different film thickness.

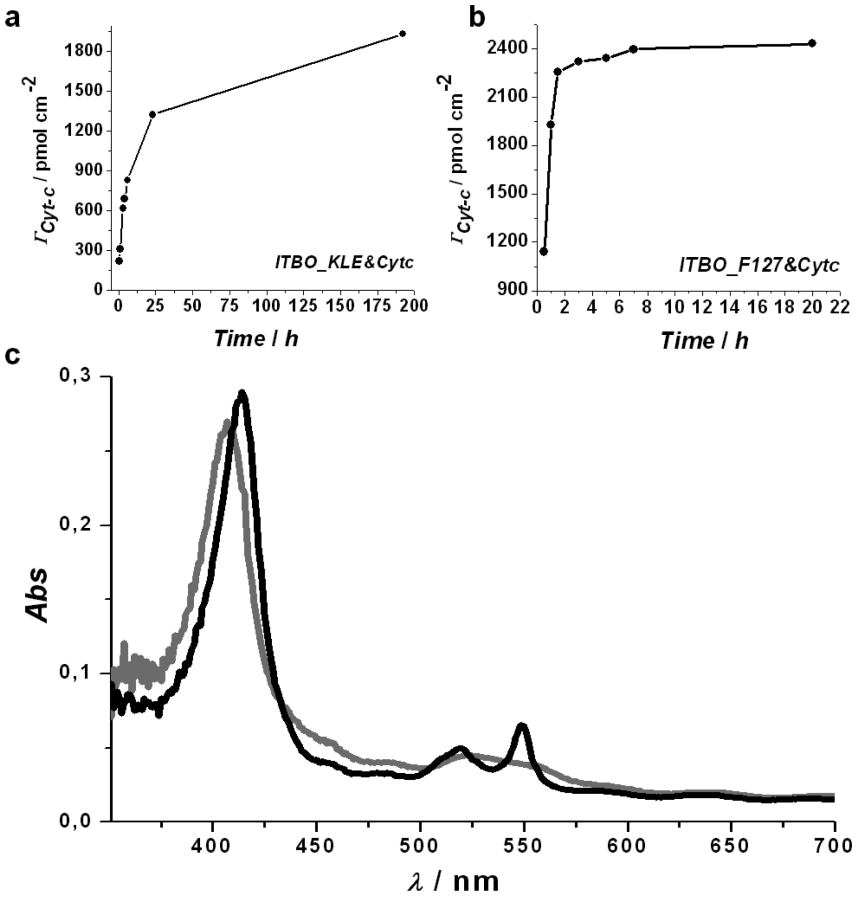

Figure 4. Cytochrome c surface loading of (a) ITO_KLE and (b) ITO_F127 for different protein incubation times in a 15 μM cytochrome c solution determined spectroscopically in protein-free potassium phosphate buffer (5 mM, pH 7.0). (c) Absorption spectra of Cyt c adsorbed on a mpITBO_F127 electrode at +0.2 V (gray line) and at −0.2 V (black line) vs Ag/AgCL/1 M KCl, corresponding to the ferric and ferrous form of Cyt c, respectively.

The increase of the protein amount in thicker films is a clue of the effective deep localization of the protein inside the three-dimensional structure. The cytochrome c incorporation takes much more time for ITBO_KLE than for ITBO_F127 (Figure 4). For ITBO_KLE it takes about a week to reach a maximum amount of immobilized protein, whereas for ITBO_F127 the maximum amount is reached in less than 2 h. It should be noted that for the two templates the formation of different mesostructures in silicas have been reported. For KLE the formation of close-packed spherical pores connected via smaller micropores was reported,[30] while for F127 typically a two-dimensional hexagonal arrangement of cylindrical pores is found.[49] Although the mesostructures reported here do not exhibit long-range periodicity, from the TEM pictures also the formation of spherical and cylindrical ("worm-like") pores can be observed in ITBO_KLE and ITBO_F127, respectively. Thus, although ITBO_KLE possesses a larger mesopore diameter, the pores are harder to access for the protein, as the connectivities between those pores are much smaller.

In both cases the finally immobilized cytochrome c is able to exchange electrons directly with the conductive electrode material. Cathodization (−0.3 V vs Ag/AgCL/1 M KCl) of the modified electrode, for a couple of minutes, reduces completely the present protein, within the margins of error. In the same way cytochrome c is reoxidized, applying a positive potential around 300 mV. This process is fully reversible and thus can be exploited to study the protein in a potentiostatically controlled redox state. The optical properties of ITBO allow monitoring of the state of cytochrome c by UV/vis simultaneously with electrochemistry. The oxidation state of the immobilized cytochrome c was reversibly switched from the ferric to the ferrous form upon varying the electrode potential between +0.2 and −0.2 V (vs AgAgCl/1 M KCl). Oxidized and reduced cytochrome c display characteristic absorption spectra. The switch from oxidized (ferric) to reduced (ferrous) state is indicated by the shift of the Soret band from 410 to 416 nm and the evolution of the 520 and 550 nm bands in the Q-band region (Figure 4c).

CONCLUSION

In conclusion, we demonstrated for the first time that mesoporous, tin-rich ITO films with durable and high electrical conductivity can be prepared directly from a hetero-bimetallic single-source ITBO precursor in solution. The addition of polymer additives yields an accessible and tailorable porosity while maintaining the conductivity and optical transparency of the coated films. TEM investigations show that the amorphous character of the conducting films is maintained even at 400 °C, which is essential for applications in printable electronics. In addition, the reduced indium concentration in the material combined with the stability of the porous structure opens the way to develop low-cost and mechanically more flexible optoelectronic

devices, solar cells, and sensors. Compared to flat commercial ITOs, the mesoporous ITOs can be loaded with higher amounts of electroactive biomolecules such as proteins. It was shown that a fast and efficient electron exchange between the inorganic host and the protein occurs in these systems. The here presented mesoporous tin-rich ITOs thus represent a promising electrode material for the development of bioelectronic devices .

■ ASSOCIATED CONTENT

Supporting Information. Photographs of mesoporous tin-rich ITO-based coatings on glass. UV−vis spectra, X-ray elemental mapping, and TEM and SEM micrographs of mesoporous tin-rich ITO films. Nitrogen sorption isotherms of mesoporous tin-rich ITOs calcined at different temperatures. This material is available free of charge via the Internet at http://pubs.acs.org.

■ AUTHOR INFORMATION

Corresponding Author

*E-mail: arne.thomas@tu-berlin.de; matthias.driess@tu-berlin.de.

■ ACKNOWLEDGMENT

Financial support from the Cluster of Excellence "Unifying Concepts in Catalysis" (supported by the Deutsche Forschungsgemeinschaft and administered by the TU Berlin) is gratefully acknowledged. We thank Dr. Kamalakannan Kailasam for help with the analysis of the materials. We acknowledge the help of Sören Selve and the ZELMI at TU Berlin for help with the TEM measurements.

■ REFERENCES

(1) Sayari, A.; Liu, P. *Microporous Mater.* **1997**, *12*, 149.
(2) Schuth, F. *Chem. Mater.* **2001**, *13*, 3184.
(3) Soler-Illia, G.; Crepaldi, E. L.; Grosso, D.; Sanchez, C. *Curr. Opin. Colloid Interface Sci.* **2003**, *8*, 109.
(4) Brinker, C. J.; Dunphy, D. R. *Curr. Opin. Colloid Interface Sci.* **2006**, *11*, 126.
(5) Kondo, J. N.; Domen, K. *Chem. Mater.* **2008**, *20*, 835.
(6) Chopra, K. L.; Major, S.; Pandya, D. K. *Thin Solid Films* **1983**, *102*, 1.
(7) Ginley, D. S.; Bright, C. *MRS Bull.* **2000**, *25*, 15.
(8) Lin, H.; Jin, T.; Dmytruk, A.; Saito, M.; Yazawa, T. *J. Photochem. Photobiol., A* **2004**, *164*, 173.
(9) Dong, J. Q.; Gafney, H. D. *J. Non-Cryst. Solids* **1996**, *203*, 329.
(10) Zhang, Q.; Zhu, M. F.; Zhang, Q. H.; Li, Y. G.; Wang, H. Z. *J. Phys. Chem. C* **2009**, *113*, 15538.
(11) Emons, T. T.; Li, J. Q.; Nazar, L. F. *J. Am. Chem. Soc.* **2002**, *124*, 8516.
(12) Stoica, T. F.; Gartner, M.; Stoica, T.; Losurdo, M.; Teodorescu, V. S.; Blanchin, M. G.; Zaharescu, M. *J. Optoelectron. Adv. Mater.* **2005**, *7*, 2353.
(13) Daoudi, K.; Canut, B.; Blanchin, M. G.; Sandu, C. S.; Teodorescu, V. S.; Roger, J. A. *Thin Solid Films* **2003**, *445*, 20.
(14) Fattakhova-Rohfing, D.; Brezesinski, T.; Rathousky, J.; Feldhoff, A.; Oekermann, T.; Wark, M.; Smarsly, B. *Adv. Mater.* **2006**, *18*, 2980.
(15) Wang, Y. D.; Brezesinski, T.; Antonietti, M.; Smarsly, B. *ACS Nano* **2009**, *3*, 1373.
(16) Frasca, S.; von Graberg, T.; Feng, J. J.; Thomas, A.; Smarsly, B.; Weidinger, I.; Scheller, F.; Hildebrandt, P.; Wollenberger, U. *ChemCatChem* **2010**, *2*, 839.
(17) Muller, V.; Rasp, M.; Rathousky, J.; Schutz, B.; Niederberger, M.; Fattakhova-Rohlfing, D. *Small* **2010**, *6*, 633.
(18) Frank, G.; Kostlin, H. *Appl. Phys. A-Mater. Sci. Process* **1982**, *27*, 197.
(19) Aksu, Y.; Driess, M. *Angew. Chem., Int. Ed.* **2009**, *48*, 7778.
(20) Arndt, S.; Aksu, Y.; Driess, M.; Schomäcker, R. *Catal. Lett.* **2009**, *131*, 258.
(21) Heitz, S.; Aksu, Y.; Driess, M. *Chem. Mater.* **2010**, *22*, 1376.
(22) Jana, S.; Aksu, Y.; Driess, M. *Dalton Trans.* **2009**, 1516.
(23) Ma, J.-G.; Aksu, Y.; Gregoriades, L. J.; Sauer, J.; Driess, M. *Dalton Trans.* **2010**, *39*, 103.
(24) Polarz, S.; Orlov, A.; Hoffmann, A.; Wagner, M. R.; Rauch, C.; Kirste, R.; Gehlhoff, W.; Aksu, Y.; Driess, M.; Berg, M. W. E. v. d.; Lehmann, M. *Chem. Mater.* **2009**, *21*, 3889.
(25) Rauch, C.; Gehlhoff, W.; Wagner, M. R.; Malguth, E.; Callsen, G.; Kirste, R.; Salameh, B.; Hoffmann, A.; Polarz, S.; Aksu, Y.; Driess, M. *J. Appl. Phys.* **2010**, *107*, 024311.
(26) Veith, M.; Kunze, K. *Angew. Chem., Int. Ed.* **1991**, *30*, 95.
(27) Nicholson, R. S. *Anal. Chem.* **1965**, *37*, 1351.
(28) Topoglidis, E.; Cass, A. E. G.; Gilardi, G.; Sadeghi, S.; Beaumont, N.; Durrant, J. R. *Anal. Chem.* **1998**, *70*, 5111.
(29) Collinson, M.; Bowden, E. F. *Anal. Chem.* **1992**, *64*, 1470.
(30) Thomas, A.; Schlaad, H.; Smarsly, B.; Antonietti, M. *Langmuir* **2003**, *19*, 4455.
(31) Brezesinski, T.; Antonietti, M.; Groenewolt, M.; Pinna, N.; Smarsly, B. *New J. Chem.* **2005**, *29*, 237.
(32) Grosso, D.; Boissiere, C.; Smarsly, B.; Brezesinski, T.; Pinna, N.; Albouy, P. A.; Amenitsch, H.; Antonietti, M.; Sanchez, C. *Nat. Mater.* **2004**, *3*, 787.
(33) Smarsly, B.; Grosso, D.; Brezesinski, T.; Pinna, N.; Boissiere, C.; Antonietti, M.; Sanchez, C. *Chem. Mater.* **2004**, *16*, 2948.
(34) Thomas, A.; Schierhorn, M.; Wu, Y. Y.; Stucky, G. *J. Mater. Chem.* **2007**, *17*, 4558.
(35) (a) Leite, E. R; Bernardi, M. I. B.; Longo, E.; Varela, J. A.; Paskocimas, C. A. *Thin Solid Films* **2004**, *449*, 67–72. (b) Alam, M. J.; Cameron, D. C. *Thin Solid Films* **2002**, *420*, 76.
(36) Guillen, C.; Herrero, J. *Thin Solid Films* **2006**, *510*, 260.
(37) Jung, Y. S. *Solid State Commun.* **2004**, *129*, 491.
(38) Topoglidis, E.; Cass, A. E. G.; O'Regan, B.; Durrant, J. R. *J. Electroanal. Chem.* **2001**, *517*, 20.
(39) Topoglidis, E.; Lutz, T.; Durrant, J. R.; Palomares, E. *Bioelectrochemistry* **2008**, *74*, 142.
(40) Topoglidis, E.; Discher, B. M.; Moser, C. C.; Dutton, P. L.; Durrant, J. R. *Chembiochem* **2003**, *4*, 1332.
(41) Topoglidis, E.; Astuti, Y.; Duriaux, F.; Gratzel, M.; Durrant, J. R. *Langmuir* **2003**, *19*, 6894.
(42) Feng, J. J.; Xu, J. J.; Chen, H. Y. *Electrochem. Commun.* **2006**, *8*, 77.
(43) Feng, J. J.; Zhu, J. T.; Xu, J. J.; Chen, H. Y. *J. Nanosci. Nanotechnol.* **2009**, *9*, 2290.
(44) Rusling, J. F.; Wang, B.; Yun, S. E. *Handbook of Bioelectrochemistry: Fundamentals, Experimental Techniques and Application*; Wiley: Chichester, 2008.
(45) Scheller, F. W.; Wollenberger, U.; Lei, C.; Jin, W.; Ge, B.; Lehmann, C.; Lisdat, F.; Fridman, V. *Rev. Mol. Biotechnol.* **2002**, *82*, 411.
(46) Beissenhirtz, M. K.; Scheller, F. W.; Stocklein, W. F. M.; Kurth, D. G.; Mohwald, H.; Lisdat, F. *Angew. Chem., Int. Ed.* **2004**, *43*, 4357.
(47) Murata, K.; Kajiya, K.; Nukaga, M.; Suga, Y.; Watanabe, T.; Nakamura, N.; Ohno, H. *Electroanalysis* **2010**, *22*, 185.
(48) Milliron, D. J.; Hill, I. G.; Shen, C.; Kahn, A.; Schwartz, J. *J. Appl. Phys.* **2000**, *87*, 572.
(49) Grosso, D.; Balkenende, A. R.; Albouy, P. A.; Ayral, A.; Amenitsch, H.; Babonneau, F. *Chem. Mater.* **2001**, *13*, 1848.